Synthesis and Application of a Bidentate Ligand Based on Decafluoro-3-phenyl-3-pentanol: Steric Effect of Pentafluoroethyl Groups on the Stereomutation of *O*-Equatorial *C*-Apical Spirophosphoranes

Xin-dong Jiang[†], Ken-ichiro Kakuda[†], Shiro Matsukawa[§], Hideaki Yamamichi[†], Satoshi Kojima[†], Yohsuke Yamamoto*[†]

† *Department of Chemistry*, *Graduate School of Science*, *Hiroshima University*, *1-3-1 Kagamiyama*, *Higashi-hiroshima 739-8526*, *Japan*

Fax: *+81-82-424-0723*, Email: yyama@sci.hiroshima-u.ac.jp

§ *Institute for Advanced Materials Research, Hiroshima University, 1-3-1 Kagamiyama, Higashi-hiroshima 739-8530*, *Japan*

Abstract: 1,1,1,2,2,4,4,5,5,5-Decafluoro-3-phenyl-3-pentanol (**13**) was prepared via the Cannizzaro-type disproportionation reaction, and dimetallated **13** (i.e., **15**) was used as a bidentate ligand, which was bulkier than the Martin ligand (1,1,1,3,3,3-hexafluoro-2-phenyl-2-propanol). P-H

spirophosphorane (**16**) was synthesized utilizing the new bidentate ligand, and the structure of **16** was essentially the same as that of the P-H phosphorane with the Martin ligands (**1b**). Phosphoranes which exhibit reversed apicophilicity (**9**: *O-equatorial*) were also synthesized and could be converted to the corresponding stable stereoisomers (**10**: *O-apical*). The crystal structures of *O-equatorial* phosphoranes (**9**) and those of *O-apical* isomers (**10**) were slightly affected by the steric repulsion of pentafluoroethyl groups. Kinetic measurements revealed that the stereomutation of *O-equatorial* methylphosphorane (**9a**) to the *O-apical* isomer (**10a**) was slowed. The activation enthalpy for the stereomutation of **9a→10a** (24.4 kcal mol^{-1}) was higher than that of the phosphorane bearing the Martin ligands (**3a→4a**: 19.3 kcal mol^{-1}) by 5.1 kcal mol^{-1}.

Introduction

Hypervalent phosphorus compounds[1] have attracted great interest because such species are assumed to be involved as intermediates (or transition states) in the biological phosphoryl transfer reaction.[2] According to the Westheimer rule,[2d] in phosphoryl transfer reactions, a nucleophile attacks a phosphoryl center to give a pentacoordinate intermediate which bears the

nucleophile at the apical position, then one of the two apical ligands is released to be a nucleofuge. During this reaction, if the intermediate has enough lifetime, it can easily undergo stereomutation to furnish an equilibrium mixture containing several stereoisomers: therefore, this can highly affect the product distribution. Thus, to clarify the mechanism of such reactions, comprehensive knowledge on the thermodynamic and kinetic properties of transient species would be needed; therefore, it is quite important to understand the difference in structure and reactivity of isomeric phosphoranes.

Pentacoordinate (10-P-5)[3] phosphoranes generally prefer a trigonal-bipyramidal (TBP) structure, which bears two distinct bonds (apical and equatorial). The apical bond is described as a three center-four electron (hypervalent) bond, whereas the equatorial bond is described as an sp^2 bond. Because of the distinct sites and bonds existing in the TBP structure, two characteristic properties, apicophilicity (a thermodynamic property) and pseudorotation (a kinetic property), play important roles in hypervalent phosphorane chemistry. Apicophilicity is the relative preference of a ligand occupying the apical site, and many experimental studies[4] and theoretical calculations[5] clarified that electronegative and sterically small groups prefer to occupy the apical sites while electron-donative and bulkly ligands prefer the equatorial sites. However, TBP molecules generally

isomerize in solution by a mechanism called "Berry pseudorotation (BPR)",[6] causing rapid exchange between the apical and the equatorial ligands.[7] The barrier to BPR is usually very low (calculated to be ca. 2-3 kcal mol^{-1} for PH_5[8]) without any steric restrictions.

It has been found that the Martin ligand, which forms a rigid five-membered ring, stabilizes many kinds of hypervalent compounds both thermodynamically and kinetically.[9] Utilizing the Martin ligand, we succeeded in isolating enantiomeric pairs of optically active 10-P-5 hydrophosphoranes **1**-$\boldsymbol{S_P}$ and **1**-$\boldsymbol{R_P}$, indicating that the stereomutation between **1**-$\boldsymbol{S_P}$ and **1**-$\boldsymbol{R_P}$ was sufficiently frozen to permit isolation at room temperature (Scheme 1).[10] Furthermore, we isolated phosphoranes having an apical oxygen-equatorial carbon array (**3**: *O-equatorial*) as the major product via a thermal cyclization reaction of monocyclic P-H_{apical} phosphoranes **2** (Scheme 2-a). This showed the first isolated example of a phosphorane which violates the apicophilicity concept and can still be converted to its more stable stereoisomer **4**, having two oxygen atoms at the apical sites (*O-apical*).[11] However, this method usually provides a mixture of **3** and **4**, and therefore is not the best way to prepare *O-equatorial* phosphoranes (**3**) that may undergo stereomutation around these temperatures. We later found that the *O-equatorial* phosphoranes were exclusively prepared at

lower than ambient temperature by oxidative cyclization of the dianionic phosphoranes using I_2 (Scheme 2-b).[12] *O-equatorial* phosphorane with a bulky aryl group (2,4,6-triisopropylphenyl) was also isolated by the same method. These *O-equatorial* phosphoranes isomerized irreversibly to their stable stereoisomers (*O-apical*) at elevated temperatures, indicating that the *O-equatorial* isomers were kinetic products. There are several examples of isolated phosphoranes exhibiting "reversed apicophilicity".[5i-k,13,14] It is notable that, by introducing very bulky bidentate ligand, some of those phosphoranes become thermodynamically stable species even though the regular configulations are allowed, and a new insight on the apicophilicity has been unveiled from the unique system.[5i-k,14]

<Scheme 1>

<Scheme 2>

Successful isolation of several pairs of *O-equatorial* and *O-apical* phosphoranes led us to investigate the difference in structure and reactivity of these stereoisomers. We found that *O-equatorial* phosphoranes (**3**) easily reacted with nucleophiles, whereas *O-apical* isomers (**4**) did

not react at all under similar conditions and that the α-carbanion (**5**) derived from *O-equatorial* isomer was stablized by the $n_C \rightarrow \sigma^*_{P\text{-}O}$ interaction, which was supported by the theoretical calculations.[15] Moreover, *O-equatorial* phosphoranes (**7**) bearing a primary amino group were also isolated, and the energy of the $n_N \rightarrow \sigma^*_{P\text{-}O}$ interaction was quantitatively estimated to be ca. 4 kcal mol^{-1} based on the kinetic measurements and theoretical calculations.[16]

<Figure 1>

As shown above, we succeeded in clarifying the property differences between isomeric phosphoranes, of which BPR was efficiently frozen by the use of the Martin ligand. However, we have not been successful in isolating phosphoranes bearing small or electronegative substituents as the equatorial monodentate ligand. For example, the stereomutation of *O-equatorial* methylphosphorane (**3a**) to the *O-apical* isomer (**4a**) was relatively fast even at room temperature; therefore, **3a** could not be isolated in pure form. That is, to isolate a phosphorane with a small or electronegative group at the equatorial site, a bidentate ligand which suppresses BPR more

efficiently than the Martin ligand should be needed.

In this article, we present the synthesis of a new bidentate ligand bearing two pentafluoroethyl (C_2F_5) groups, which is bulkier than the Martin ligand (Figure 2). The key reaction of the synthesis is a Cannizzaro-type disproportionation involving intermolecular migration of the pentafluoroethyl group. The synthesis and structures of *O-equatorial* phosphoranes (**9**) bearing the bidentate ligands will then be discussed. The crystal structure of **9** was found to be slightly different from the phosphoranes with the Martin ligands (**3**). A kinetic study of the stereomutation of a methyl derivative (**9a** to **10a**) revealed that the steric bulkiness of the C_2F_5 group actually raised the energy barrier to pseudorotation. Full details are shown herein.

<Figure 2>

Results and Discussion

Synthesis of 1,1,1,2,2,4,4,5,5,5-decafluoro-3-phenyl-3-pentanol (13) via the Cannizzaro-type reaction and the ligand precursor 14. Recently, two different methods for the synthesis of

1,1,1,2,2,4,4,5,5,5-decafluoro-3-phenyl-3-pentanol (**13**) utilizing C_2F_5I were reported.[17] In these methods, however, the boiling point of C_2F_5I is so low (12–13 ˚C) that the experimental operation becomes troublesome. Therefore, we exploited a new synthetic method obtaining the alcohol **13** and found that the Cannizzaro-type reaction[18] was convenient. At first, pentafluoropropiophenone (**12**) was prepared from ethyl pentafluoropropionate **(11**) with PhLi in 84% yield (Scheme 3). As reported previously, trifluoroacetophenone functions as a trifluoromethyl anion source in the presence of *t*BuOK.[19] Therefore, we examined the use of this methodology for the synthesis of **13**. As expected, treatment of **12** with 0.5 equiv. of *t*BuOK in THF furnished the desired alcohol **13** in 33% yield (66% based on the C_2F_5 group). The reaction proceeded cleanly at room temperature, and the by-product, *tert*-butyl benzoate, was easily removed from **13** by treatment with trifluoroacetic acid. To our knowledge, this is the first example of a Cannizzaro-type disproportionation of a perfluoroalkyl group.

For the Martin ligand, it is known that hexafluorocumyl alcohol is quantitatively dilithiated with a stoichiometric amount of *n*BuLi in the presence of a catalytic amount of TMEDA (N,N,N',N'-tetramethylethylenediamine).[20] However, in the present case, dilithiation of the alcohol

13 was not completed (up to 70%) by the same method. We found that 3 equivalents of *n*BuLi/TMEDA were needed for complete dilithiation of **13**. Therefore, **13** was converted to *o*-bromo derivative **14** in 84% yield, which was used as the precursor of the bidentate ligand (Scheme 3).

<Scheme 3>

Dimetallation of 14 and synthesis of P-H Spirophosphorane 16. At first, dimetallation of **14** was examined (Scheme 4). Compound **14** was treated with 2.2 equiv. of *n*BuLi followed by D_2O; partially deuterated **13** was produced (**13-D** : **13** = 33 : 67). From this result, the lithium-bromine exchange reaction using *n*BuLi was clearly faster than the hydroxyl proton abstraction. Thus, the resulting aryllithium generated from the reaction of *n*BuLi with **14** was readily quenched by intramolecular proton transfer from the alcohol functionality. To avoid the intramolecular proton transfer, the combined system, NaH followed by *n*BuLi (or *t*BuLi), was employed. Based on the ^1H NMR spectrum, the bromine atom was found to be completely replaced with deuterium. This

condition should be good in view of the reactivity of the dianion **15** and should be suitable for large scale synthesis.

<Scheme 4>

The dianion **15**, completely generated from **14** with the combined system of NaH and *n*BuLi as described above, was added to a THF solution of PCl_3 to give P-H spirophosphorane **16** (50%) along with *O-apical n*-butylphosphorane **10b** (6%) (Scheme 5). The latter was provided by the reaction of the intermediate phosphoranide anion with *n*BuBr which was formed during the dimetallation process. This problem was easily solved by the use of *t*BuLi instead of *n*BuLi, giving only **16** in 35% yield. The structure of phosphorane **16** was confirmed by X-ray analysis and was regarded as a trigonal bipyramidal (TBP) structure (Figure 3). Compared with the reported P-H spirophosphorane **1b**[21] bearing the Martin ligands, the C1—P1—C2 angle of **16** (136.3°) in the equatorial plane was larger by 8.7° than that of **1b** (127.6°). This should be due to the steric repulsion between the bulky *endo*-C_2F_5 groups and the aromatic rings.

<Scheme 5>

<Figure 3>

Synthesis of *O-equatorial* spirophosphoranes (9). The *O-equatorial* phosphoranes **9a**, **9b** and **9c** were prepared from the reaction of P-H phosphorane **16** with 3 equiv. of RLi followed by treatment with I_2.[12] All the *O-equatorial* phosphoranes were almost quantitatively converted to the corresponding *O-apical* phosphoranes by heating in solution (Scheme 6). It is noted that *O-equatorial* isomer **9a** is isolated in pure form in the case of the methyl derivative. This obviously indicates that stereomutation of **9a** to **10a** is sufficiently suppressed to permit isolation. The trend of ^{31}P NMR, i.e., *O-equatorial* {δ = –4.7 (**9a**), –1.5 (**9b**) and 11.2 (**9c**) ppm in $CDCl_3$} is shifted downfield compared with *O-apical* {δ = –21.2 (**10a**), –16.1 (**10b**) and –3.2 (**10c**) ppm in $CDCl_3$}, is the same as that for the CF_3 derivatives (**3** and **4**).[11b]

<Scheme 6>

<Figure 4>

<Table 1>

The structures of phosphoranes **9a**-**9c**, **10a** and **10b** were confirmed by X-ray analysis (Figure 4 and Table 1), showing that all the structures were regarded as slightly distorted trigonal bipyramidal (TBP) geometry.[22] We found that the steric bulkiness of the pentafluoroethyl groups slightly affected the crystal structures by comparing CF_3 derivatives (**3b** and **4b**) and the C_2F_5 derivatives (**9b** and **10b**) as shown in Figure 5 and Table 1. As for the *O-apical* phosphoranes **4b** and **10b**, the apical P—O distances {1.763(1) and 1.754(1) Å for **4b**, 1.759(3) and 1.750(3) Å for **10b**} were very similar, and the C1—P1—C2 angle of **10b** (134.28˚) is expanded by 7.3˚ compared with that of **4b** (127.0˚). This should be due to steric repulsion between the *endo*-C_2F_5 group and the equatorial aromatic ring. On the other hand, in the *O-equatorial* phosphoranes **3b**[11a] and **9b**, the apical P1—O1 bond of **9b** {1.800(2) Å} is longer than the corresponding bond of **3b** {1.770(3) Å} by 0.03 Å. Because CF_3 groups are small, the steric hindrance in **3b** should be negligible. However, steric repulsion between the *endo*-C_2F_5 groups of **9b** would be inevitable; therefore, the apical

P1—O1 bond of **9b** is forced to become somewhat elongated compared with that of **3b**. Other structural parameters for **3b** and **9b** around the phosphorus were very similar.

<Figure 5>

Kinetic study of the isomerization of *O-equatorial* 9a to *O-apical* 10a. Successful isolation of **9a** shows its high stability at room temperature; therefore, we further discuss the stereomutation of **9a** on the basis of a kinetic study. Figure 6 shows a representative example of the stereomutation monitored by ^{1}H NMR. The rate of isomerization of **9a** to **10a** was measured in C_6D_6 in the temperature range 323-343 K by monitoring the change in the ^{1}H NMR integrals of the methyl group. The measurements obey first-order kinetics. The activation parameters obtained from the Eyring plot are as follows: $\Delta S^{\neq} = -5.1 \pm 2.4$ e.u., $\Delta H^{\neq} = 24.4 \pm 0.8$ kcal mol^{-1}, $\Delta G^{\neq}_{333} = 26.1$ kcal mol^{-1} (Figure 7). The activation free energy for the steromutation of **9a** to **10a** was actually higher than that of **3a** to **4a** ($\Delta G^{\neq}_{333} = 22.5$ kcal mol^{-1})[16] by 3.6 kcal mol^{-1}, indicating that the steric effect of the C_2F_5 group was more effective for freezing pseudorotation than the CF_3 group.

<Figure 6>

<Figure 7>

<Scheme 7>

As previously proposed by our group,[11] isomer **17a**, which bears one of the two bidentate ligands at the diequatorial sites, would be the highest isomer in energy; therefore, the structure of this isomer is assumed to be similar to the actual transition state (**TS**) for the stereomutation (Scheme 7). The difference in the activation enthalpy ($\Delta H^{\neq}$ = 19.3 kcal mol^{-1} for **3a** to **4a**,[16] 24.4 kcal mol^{-1} for **9a** to **10a**) mainly contributes to the difference in the activation free energy. This could mean that the steric repulsion between the Rf group and the aromatic ring of the diequatorial bidentate ligand in **18a** (Rf = C_2F_5) is larger than that of **17a** (Rf = CF_3), causing the new bidentate ligand bearing C_2F_5 groups to be more effective in freezing pseudorotation than the Martin ligand.

Conclusions

1,1,1,2,2,4,4,5,5,5-Decafluoro-3-phenyl-3-pentanol (**13**) was synthesized via the Cannizzaro-type reaction in 28% overall yield. During the examination of the dimetallation of **14**, it was found that the lithium-bromine exchange reaction was faster than the hydroxyl proton abstraction with the use of *n*BuLi. This problem was easily resolved by using the combined system, NaH followed by *n*BuLi (or *t*BuLi). Using the dianion **15**, P-H spirophosphorane **16** was obtained in a moderate yield of 50%. The *O-equatorial* phosphoranes **9** were synthesized and successfully isolated. By the X-ray analysis, steric repulsion between the *endo*-C_2F_5 groups slightly affected the structure, leading the apical P1—O1 bond to be forced to elongate in *O-equatorial* phosphorane **9b** compared with CF_3 derivative **3b**. The kinetic study revealed that the steric hindrance of the C_2F_5 group was more effective for freezing pseudorotation than the CF_3 group. Further synthetic studies of hypervalent compounds utilizing the new bidentate ligand are ongoing.

Experimental Section

General: Melting points were measured using a Yanaco micro melting point apparatus. ^{1}H NMR (400 MHz), ^{19}F NMR (376 MHz), and ^{31}P NMR (162 MHz) were recorded using a JEOL EX-400

or a JEOL AL-400 spectrometer. ^{1}H NMR chemical shifts (δ) are given in ppm downfield from Me_4Si, determined by residual chloroform (δ 7.26). ^{19}F NMR chemical shifts (δ) are given in ppm downfield from external $CFCl_3$. ^{31}P NMR chemical shifts (δ) are given in ppm downfield from external 85% H_3PO_4. The elemental analyses were performed using a Perkin-Elmer 2400 CHN elemental analyzer. All reactions were carried out under N_2 or Ar. Tetrahydrofuran (THF) and diethyl ether (Et_2O) were freshly distilled from Na-benzophenone, *n*-hexane was distilled over Na, and other solvents were distilled over CaH_2. Merck silica gel 60 was used for the column chromatography.

2,2,3,3,3-Pentafluoropropiophenone (12): Under N_2, PhLi (1.05 M cyclohexane-Et_2O solution, 100 mL, 105 mmol) was added to a solution of ethyl pentafluoropropionate **7** (17.9 g, 93.4 mmol) in THF (224 mL) at –78 ˚C and the mixture was stirred for 2 h at the same temperature. The reaction mixture was then treated with 2 M HCl (60 mL) at –78 ˚C and stirred for 10 h at room temperature. The mixture was extracted with Et_2O (150 mL × 2), and the organic layer was washed with brine (80 mL × 2) and dried over anhydrous $MgSO_4$. After removing the solvents by evaporation, the yellow oil was subjected to distillation to afford a colorless liquid of **12** (17.6 g,

78.7 mmol, 84%). B.p.: 61.2-62.0 ˚C/26 mmHg (lit[17a] 76-78 ˚C/29 mmHg). ^{1}H NMR ($CDCl_3$): δ = 8.09 (d, $^3J_{H\text{-}H}$ = 8 Hz, 2H), 7.72 (t, $^3J_{H\text{-}H}$ = 8 Hz, 1H), 7.55 (t, $^3J_{H\text{-}H}$ = 8 Hz, 2H) ppm. ^{19}F NMR ($CDCl_3$): δ = –82.0 (s, 3F), –116.0 (s, 2F) ppm.

1,1,1,2,2,4,4,5,5,5-Decafluoro-3-phenyl-3-pentanol (13): Under N_2, *t*BuOK (1.0 M THF solution, 12.5 mL, 12.5 mmol) was added to a solution of **12** (5.51 g, 24.6 mmol) in THF (50 mL) at 0 ˚C and the mixture was stirred for 15 h at room temperature. After removing the solvents by evaporation, CH_2Cl_2 (5.6 mL) was added. Trifluoroacetic acid (7.5 mL, 101 mmol) was added to the mixture at 0 ˚C and the mixture was stirred for 60 h at room temperature. The reaction was quenched with saturated aqueous Na_2CO_3 (80 mL). The mixture was extracted with Et_2O (100 mL × 2), and the organic layer was washed with brine (50 mL × 2) and dried over anhydrous $MgSO_4$. After removing the solvents by evaporation, the yellow oil was separated by column chromatography (CH_2Cl_2 : *n*-hexane : benzene = 1 : 6 : 0.21), and followed by distillation to afford a colorless liquid of **13** (2.86 g, 8.30 mmol, 33%). B.p.: 35.0-36.0 ˚C/0.7 mmHg (lit[17a] 55-56 ˚C/4 mmHg). ^{1}H NMR ($CDCl_3$): δ = 7.72 (d, $^3J_{H\text{-}H}$ = 7.6 Hz, 2H), 7.42-7.47 (m, 3H), 3.57 (br s, 1H) ppm. ^{19}F NMR ($CDCl_3$): δ = –78.0 (s, 6F), –116.3 (d, $^2J_{F\text{-}F}$ = 278 Hz, 2F), –120.1 (d, $^2J_{F\text{-}F}$ = 278 Hz, 2F) ppm.

FAB-MS: (*m*/*z*) 344 (M^+), 327 (M^+–OH), 225 (M^+–C_2F_5).

1,1,1,2,2,4,4,5,5,5-Decafluoro-3-(2-bromophenyl)-3-pentanol (14): Under Ar, to *n*BuLi (1.59 M *n*-hexane solution, 9.20 mL, 14.6 mmol) was added TMEDA (N,N,N',N'-tetramethylethylenediamine: 2.20 mL, 14.6 mmol) at room temperature and the mixture was stirred for 30 minutes. Compound **13 (**1.68 g, 4.88 mmol) was then added to the mixture at 0 ˚C and stirred for 36 h at room temperature. 1,2-Dibromo-1,1,2,2-tetrafluoroethane (2.60 mL, 21.8 mmol) was added at –78 ˚C and stirred for 3 h at room temperature. The reaction was quenched with 2 M HCl (40 mL) at 0 ˚C. The mixture was extracted with Et_2O (50 mL × 2), and the organic layer was washed with brine (30 mL × 2) and dried over anhydrous $MgSO_4$. After removing the solvents by evaporation, the yellow oil was separated by column chromatography (CH_2Cl_2 : *n*-hexane : benzene = 1 : 6 : 0.21), and followed by distillation to afford a colorless liquid of **14 (**1.73 g, 4.09 mmol, 84%). B.p.: 66.0-67.0 ˚C/0.7 mmHg. ^{1}H NMR ($CDCl_3$): δ = 7.75 (br d, $^3J_{H\text{-}H}$ = 8 Hz, 1H), 7.69 (dd, $^3J_{H\text{-}H}$ = 8 Hz, $^4J_{H\text{-}H}$ = 1 Hz, 1H), 7.41 (td, $^3J_{H\text{-}H}$ = 8 Hz, $^4J_{H\text{-}H}$ = 1 Hz, 1H), 7.33 (td, $^3J_{H\text{-}H}$ = 8 Hz, $^4J_{H\text{-}H}$ = 1 Hz, 1H), 5.50 (br s, 1H) ppm. ^{19}F NMR ($CDCl_3$): δ = –78.1 (m, 6F), –116.6 (d, $^2J_{F\text{-}F}$ = 290 Hz, 2F), –117.7 (d, $^2J_{F\text{-}F}$ = 290 Hz, 2F) ppm.

[*TBPY*-5-11]-1-Hydro-3,3,3',3'-tetrakis(pentafluoroethyl)-1,1'-spirobi[3*H*,2,1,λ^5-benzoxaphosphole] (16): Under N_2, to a THF (2 mL) suspension of NaH (106 mg, 2.65 mmol) was added a solution of **14** (563 mg, 1.33 mmol) in THF (4 ml) at 0 ˚C and the mixture was stirred for 0.5 h at room temperature. The mixture was then cooled at –78 ˚C, and *n*BuLi (1.59 M *n*-hexane solution, 0.84 mL, 1.33 mmol) was added and stirred for 1 h at the same temperature. After the mixture was stirred for 1 h at room temperature, the mixture was transferred to a solution of PCl_3 (0.058 mL, 0.663 mmol) in THF (4 mL) at –78 ˚C and stirred for 0.5 h. The mixture was warmed to 0 ˚C and stirred for 1.5 h. The reaction was quenched with 6 M HCl (10 mL) at 0 ˚C. The mixture was extracted with ether (50 mL × 2), and the organic layer was washed with brine (40 mL × 2) and dried over anhydrous $MgSO_4$. After removing the solvents by evaporation, the resulting crude was separated by column chromatography (*n*-hexane) to afford white solids of **16** (238 mg, 0.333 mmol, 50 %) and **10b** (30.7 mg, 0.039 mmol, 6%). Colorless crystals of **16** and **10b** suitable for X-ray analysis were obtained by recrystallization from *n*-hexane/ether and $CHCl_3$, respectively. **16**: ^{1}H NMR ($CDCl_3$): δ = 8.41-8.36 (m, 2H), 7.96 (d, $^1J_{H\text{-}P}$ = 703 Hz, 1H), 7.81-7.72 (m, 6H) ppm. ^{19}F NMR ($CDCl_3$): δ = –78.2 (s, 6F), –79.9 (dd, $^3J_{F\text{-}F}$ = 12 Hz, $^3J_{F\text{-}F}$ = 4 Hz, 6F), –116.5 (dq, $^2J_{F\text{-}F}$ = 288

Hz, $^{3}J_{F\text{-}F}$ = 4 Hz, 2F), –117.6 (d, $^{2}J_{F\text{-}F}$ = 288 Hz, 2F), –118.5 (d, $^{2}J_{F\text{-}F}$ = 288 Hz, 2F), –120.6 (dq, $^{2}J_{F\text{-}F}$ = 288 Hz, $^{3}J_{F\text{-}F}$ = 12 Hz, 2F) ppm. ^{31}P NMR ($CDCl_3$): δ = –47.2 ppm. M.p. 135.0-136.0 ˚C. Anal. Calcd. for $C_{22}H_9F_{20}O_2P$: C 36.89, H 1.27; Found: C 36.95, H 1.56. **10b**: ^{1}H NMR ($CDCl_3$): δ = 8.47-8.41 (m, 2H), 7.75-7.66 (m, 6H), 2.19-2.00 (m, 2H), 1.15-1.26 (m, 4H), 0.75 (t, $^{3}J_{H\text{-}H}$ = 8 Hz, 3H) ppm. ^{19}F NMR ($CDCl_3$): δ = –78.5 (s, 6F), –79.6 (dd, $^{2}J_{F\text{-}F}$ = 19 Hz, $^{3}J_{F\text{-}F}$ = 6 Hz, 6F), –116.3 (d, $^{2}J_{F\text{-}F}$ = 290 Hz, 2F), –116.4 (dq, $^{2}J_{F\text{-}F}$ = 290 Hz, $^{3}J_{F\text{-}F}$ = 19 Hz, 2F), –117.4 (d, $^{2}J_{F\text{-}F}$ = 290 Hz, 2F), –120.7 (d, $^{2}J_{F\text{-}F}$ = 290 Hz, 2F) ppm. ^{31}P NMR ($CDCl_3$): δ = –16.1 ppm. M.p. 101.0-102.0 ˚C. Anal. Calcd. for $C_{26}H_{17}F_{20}O_2P$: C 40.43, H 2.22; Found: C 40.72, H 2.39.

[*TBPY*-5-12]-1-Methyl-3,3,3',3'-tetrakis(pentafluoroethyl)-1,1'-spirobi[3*H*,2,1,λ^5-benzoxaphosphole] (9a): Under Ar, to a solution of **16** (104 mg, 0.145 mmol) in Et_2O (4.5 mL) was added MeLi (0.92 M diethyl ether solution, 0.45 mL, 0.414 mmol) at 0 ˚C. The mixture was then stirred for 3 h at room temperature. I_2 (110 mg, 0.439 mmol) was added to the mixture at –78 ˚C and stirred for 3 h at room temperature. The reaction was quenched with aqueous $Na_2S_2O_3$ (20 mL). The mixture was extracted with Et_2O (50 mL × 2), and the organic layer was washed with brine (50 mL × 2) and dried over anhydrous $MgSO_4$. After removing the solvents by evaporation, the resulting crude was

separated by column chromatography (CH_2Cl_2 : *n*-hexane = 1 : 2) to afford a white solid of **9a** (96 mg, 0.131 mmol, 90%). Colorless crystals of **9a** suitable for X-ray analysis were obtained by recrystallization from CH_3CN. ^{1}H NMR ($CDCl_3$): δ = 7.75 (br s, 2H), 7.70-7.60 (m, 6H), 2.23 (d, $^2J_{H\text{-}P}$ = 12 Hz, 3H) ppm. ^{19}F NMR ($CDCl_3$): δ = –79.0 (s, 12F), –115.9 (br s, 4F), –116.5 (br s, 4F) ppm. ^{31}P NMR ($CDCl_3$): δ = –4.7 ppm. M.p. 99.5-100.4 ˚C (decomp). Anal. Calcd. for $C_{23}H_{11}F_{20}O_2P$: C 37.83, H 1.52; Found: C 37.81, H 1.71.

[*TBPY*-5-12]-1-*n*-Butyl-3,3,3',3'-tetrakis(pentafluoroethyl)-1,1'-spirobi[3*H*,2,1,λ^5-benzoxaphosphole] (9b): Under Ar, to a solution of **16** (45 mg, 0.063 mmol) in Et_2O (1.3 mL) was added *n*BuLi (1.59 M *n*-hexane solution, 0.120 mL, 0.190 mmol) at 0 ˚C, and the mixture was then stirred for 3 h at room temperature. I_2 (49 mg, 0.19 mmol) was added to the mixture at –78 ˚C and stirred for 3 h at room temperature. The reaction was quenched with aqueous $Na_2S_2O_3$ (15 mL). The mixture was extracted with Et_2O (40 mL × 2), and the organic layer was washed with brine (30 mL × 2) and dried over anhydrous $MgSO_4$. After removing the solvents by evaporation, the resulting crude was separated by column chromatography (CH_2Cl_2 : *n*-hexane = 1 : 2) to afford a white solid of **9b** (45 mg, 0.058 mmol, 92%). Colorless crystals of **9b** suitable for X-ray analysis were obtained by

recrystallization from CH_3CN. ^1H NMR ($CDCl_3$): δ = 7.57-7.62 (m, 4H), 7.73-7.79 (m, 4H), 2.43-2.35 (m, 2H), 1.58-1.51 (m, 2H), 1.32-1.20 (m, 2H), 0.80 (t, $^3J_{H-H}$ = 8 Hz, 3H) ppm. ^{19}F NMR ($CDCl_3$): δ = –79.1 (br s, 12F), –116.0 (br s, 4F), –116.2 (br s, 4F) ppm. ^{31}P NMR ($CDCl_3$): δ = –1.5 ppm. M.p. 71.0-72.0 ˚C (decomp). Anal. Calcd. for $C_{26}H_{17}F_{20}O_2P$: C 40.43, H 2.22; Found: C 40.68, H 2.37.

[*TBPY*-5-12]-1-*t*-Butyl-3,3,3',3'-tetrakis(pentafluoroethyl)-1,1'-spirobi[3*H*,2,1,λ^5-benzoxaphosphole] (9c): Under Ar, to a solution of **16** (80.0 mg, 0.117 mmol) in Et_2O (3.0 mL) was added *t*BuLi (1.50 M *n*-pentane solution, 0.22 mL, 0.330 mmol) at 0 ˚C, and the mixture was then stirred for 3 h at room temperature. I_2 (82 mg, 0.32 mmol) was added to the mixture at –78 ˚C and stirred for 3 h at room temperature. The reaction was quenched with aqueous $Na_2S_2O_3$ (20 mL). The mixture was extracted with Et_2O (40 mL × 2), and the organic layer was washed with brine (30 mL × 2) and dried over anhydrous $MgSO_4$. After removing the solvents by evaporation, the resulting crude was separated by column chromatography (CH_2Cl_2 : *n*-hexane = 1 : 2) to afford a white solid of **9c** (39 mg, 0.050 mmol, 43%). Colorless crystals of **9c** suitable for X-ray analysis were obtained by recrystallization from $CHCl_3$. ^1H NMR ($CDCl_3$): δ = 8.01 (dd, $^3J_{P-H}$ = 8 Hz, $^3J_{H-H}$ = 8 Hz, 2H), 7.72

(d, $^{3}J_{H\text{-}H}$ = 8 Hz, 2H), 7.60-7.52 (m, 4H), 1.20 (d, $^{3}J_{H\text{-}P}$ = 20 Hz, 9H) ppm. ^{19}F NMR ($CDCl_3$): δ = –78.7 (br s, 12F), –112.7 (d, $^{2}J_{F\text{-}F}$ = 293 Hz, 4F), –114.9 (d, $^{2}J_{F\text{-}F}$ = 293 Hz, 2F), –116.3 (d, $^{2}J_{F\text{-}F}$ = 293 Hz, 2F) ppm. ^{31}P NMR ($CDCl_3$): δ = 11.2 ppm. M.p. 138.0-139.0 ˚C; Anal. Calcd. for $C_{26}H_{17}F_{20}O_2P$: C 40.43, H 2.22; Found: C 40.65, H 2.40.

[*TBPY*-5-11]-1-Methyl-3,3,3',3'-tetrakis(pentafluoroethyl)-1,1'-spirobi[3*H*,2,1,λ^5-benzoxaphosphole] (10a): A C_6D_6 (0.6 mL) solution of **9a** (30 mg, 0.041 mmol) was heated at 70 ˚C for 8 h. After concentration in vacuo, a white solid of **10a** was obtained (29.3 mg, 0.0401 mmol, 98%). Colorless crystals of **10a** suitable for X-ray analysis were obtained by recrystallization from $CHCl_3$. ^{1}H NMR ($CDCl_3$): δ = 8.49-8.44 (m, 2H), 7.62-7.75 (m, 6H), 1.93 (d, $^{2}J_{H\text{-}P}$ = 16 Hz, 3H) ppm. ^{19}F NMR ($CDCl_3$): δ = –78.4 (s, 6F), –79.6 (d, $^{3}J_{F\text{-}F}$ = 19.5 Hz, 6F), –115.6 (d, $^{2}J_{F\text{-}F}$ = 289 Hz, 2F), –116.2 (dq, $^{2}J_{F\text{-}F}$ = 289 Hz, $^{3}J_{F\text{-}F}$ = 19.5 Hz, 2F), –117.0 (dd, $^{2}J_{F\text{-}F}$ = 289 Hz, $^{4}J_{F\text{-}F}$ = 40.6 Hz, 2F), –121.0 (dd, $^{2}J_{F\text{-}F}$ = 289 Hz, $^{4}J_{F\text{-}F}$ = 40.6 Hz, 2F) ppm. ^{31}P NMR ($CDCl_3$): δ = –21.2 ppm. M.p. 108.0-108.8 ˚C. Anal. Calcd. for $C_{23}H_{11}F_{20}O_2P$: C 37.83, H 1.52; Found: C 37.64, H 1.39.

[*TBPY*-5-11]-1-*n*-Butyl-3,3,3',3'-tetrakis(pentafluoroethyl)-1,1'-spirobi[3*H*,2,1,λ^5-benzoxaphosphole] (10b): A C_6D_6 (0.5 mL) solution of **9b** (10.9 mg, 0.014 mmol) was heated at 80 ˚C for 12 h.

After concentration in vacuo, a white solid of **10b** was obtained (10.9 mg, 0.014 mmol, 100%). Spectral data were consistent with those of the same product obtained as the by-product in the synthesis of **16**.

[*TBPY*-5-11]-1-*t*-Butyl-3,3,3',3'-tetrakis(pentafluoroethyl)-1,1'-spirobi[3*H*,2,1,λ^5-benzoxaphosphole] (10c): A diglyme (0.5 mL) solution of **9c** (13.2 mg, 0.017 mmol) was heated at 195 ˚C for 3 weeks. The mixture was then extracted with Et_2O (10 mL × 2), and the organic layer was washed with brine (10 mL × 2) and dried over anhydrous $MgSO_4$. After concentration in vacuo, a white solid of **10c** was obtained (12.2 mg, 0.015 mmol, 92%). ^{1}H NMR ($CDCl_3$): δ = 8.43-8.38 (m, 2H), 7.69 (br s, 2H), 7.61-7.65 (m, 4H), 1.04 (d, $^3J_{H\text{-}P}$ = 20 Hz, 9H) ppm. ^{19}F NMR ($CDCl_3$): δ = –78.2 (d, $^3J_{F\text{-}F}$ = 21 Hz, 6F), –78.4 (d, $^3J_{F\text{-}F}$ = 21 Hz, 6F), –112.0 (d, $^2J_{F\text{-}F}$ = 296 Hz, 4F), –114.5 (d, $^2J_{F\text{-}F}$ = 296 Hz, 4F), –115.3 (dq, $^2J_{F\text{-}F}$ = 296 Hz, $^3J_{F\text{-}F}$ = 21 Hz, 2F), –116.1 (dq, $^2J_{F\text{-}F}$ = 296 Hz, $^3J_{F\text{-}F}$ = 21 Hz, 2F) ppm. ^{31}P NMR ($CDCl_3$): δ = –3.2 ppm. M.p. 116.3-117.0 ˚C.

Single crystal X-ray analysis of 9a-9c, 10a, 10b and 16.

For **10b**, crystals suitable for X-ray structural determination were mounted on a Mac Science MXC-κ diffractometer and irradiated with graphite-monochromated Mo-$K\alpha$ radiation (λ = 0.71073

Å) for the data collection. The lattice parameters were determined by a least-square fitting of 31 reflections with $31^\circ < 2\theta < 35^\circ$. Data were collected in the $2\theta/\omega$ scan mode. For **9a**-**9c**, **10a** and **16**, crystals suitable for the X-ray structural determination were mounted on a Mac Science DIP2030 imaging plate diffractometer and irradiated with graphite monochromated Mo-*K*α radition (λ = 0.71073 Å) for the data collection. The unit cell parameters were determined by separately autoindexing several images in each data set using the DENZO program (MAC Science).[23] For each data set, the rotation images were collected in 3 degree increments with a total rotation of 180 deg about the ϕ axis. The data were processed using SCALEPACK. The structure was solved by a direct method with the SHELX-97 program.[24] Refinement on F^2 was carried out using full-matrix leat-squares using the SHELX-97 program.[24] All non-hydrogen atoms were refined using anisotropic thermal parameters. The H1 atom of **16** was located by the differential Fourier synthesis. The hydrogen atoms were included in the refinement along with the isotropic thermal parameters. The crystallographic data are summarized in Table 2.

<Table 2>

Kinetic Measurements of the Pseudorotation of 9a to 10a: Samples (ca. 10 mg) of **9a** dissolved in C_6D_6 (0.6 mL) were sealed in a NMR tube under N_2. Kinetic measurements of the pseudorotation process were carried out on a JEOL EX-400 spectrometer by monitoring ^{1}H NMR signals in a variable temperature mode, and the specified temperatures were maintained throughout each set of measurements (error within ±1 ˚C). The observed temperatures were calibrated with the ^{1}H NMR chemical shift difference in signals of neat 1,3-propanediol (high temperature region) and MeOH (low temperature region). The data were analyzed based on first-order kinetics using the equation of $\ln (C_0/C_{\mathbf{9a}}) = kT$, in which C_0 = ratio of **9a** at $t = 0$, $C_{\mathbf{9a}}$ = ratio of **9a** at arbitrary intervals. Here $C_0 = C_{\mathbf{9a}} + C_{\mathbf{10a}}$, $C_0/C_{\mathbf{9a}} = (C_{\mathbf{9a}} + C_{\mathbf{10a}})/ C_{\mathbf{9a}} = 1 + 1/(C_{\mathbf{9a}}/C_{\mathbf{10a}})$. The ratio $C_{\mathbf{9a}}/C_{\mathbf{10a}}$ was monitored by the integration of ^{1}H NMR signals of the methyl group at 50, 55, 60, 65, and 70 ˚C. Rate constants and activation parameters for stereomutation from **9a** to **10a** are shown in Table 3.

<Table 3>

Supplementary material

CCDC-621574 (**9a**), 621575 (**9b**), 621576 (**9c**), 621577 (**10a**), 621578 (**10b**) and 621579 (**16**) contain the supplementary crystallographic data for this paper. These data can be obtained free of charge from the Cambridge Crystallographic Data Centre via www.ccdc.cam.ac.uk/data_request/cif.

Acknowledgements

This work was supported by two Grants-in-Aid for Scientific Research on Priority Areas (Nos. 14340199, 17350021) from the Ministry of Education, Culture, Sports, Science and Technology, Japan.

References

[1] a) K.-y. Akiba, *Chemistry of Hypervalent Compounds*; Wiley-VCH: New York, 1999; b) R. R. Homes, *Pentacoordinated Phosphorus — Structure and Spectroscopy*; ACS Monograph 175, 176, Vol, I, II; American Chemical Society, Washington, DC, 1980; c) D. E. C. Corbridge, *Phosphorus*: *An Outline of Its Chemistry*, *Biochemistry*, *and Technology*, 4th ed.; Elsevier:

Amsterdam, 1990, Chapter 14, pp 1233-1256; d) R. Burgada, R. Setton, In *The Chemistry of Organophosphorus Compounds*; F. R. Hartley, Ed.; Wiley-Interscience: Chichester, Great Britain, 1994, Vol. 3, pp 185-277.

[2] a) A. C. Hengge, *Acc. Chem. Res.* **2002**, *35*, 105-112, and references therein; b) S. D. Lahiri, G. Zhang, D. Dunaway-Mariano, K. N. Allen, *Science* **2003**, *299*, 2067-2071; c) R. R. Holmes, *Acc. Chem. Res.* **2004**, *37*, 746-753; d) F. H. Westheimer, *Acc. Chem. Res.* **1968**, *1*, 70-78; e) G. R. J. Thatcher, R. Kluger, *Adv. Phys. Org. Chem.* **1989**, *25*, 99-265. For recent mechanistic studies on phosphoryl transfer reaction; see f) C. S. López, O. N. Faza, A. R. de Lera, D. M. York, *Chem. Eur. J.* **2005**, *11*, 2081-2093 and references therein; g) T. Uchimaru, M. Uebayasi, T. Hirose, S. Tsuzuki, A. Yliniemelä, K. Tanabe, K. Taira, *J. Org. Chem.* **1996**, *61*, 1599-1608.

[3] For the *N*-X-*L* designation, see: C. W. Perkins, J. C. Martin, A. J. Arduengo, W. Lau, A. Alegria, J. K. Kochi, *J. Am. Chem. Soc.* **1980**, *102*, 7753-7759.

[4] a) M. Nakamoto, S. Kojima, S. Matsukawa, Y. Yamamoto, K.-y. Akiba, *J. Organometal. Chem.* **2002**, *643-644*, 441-452; b) S. Matsukawa, K. Kajiyama, S. Kojima, S.-y. Furuta, Y. Yamamoto, K.-y. Akiba, *Angew. Chem. Int. Ed.* **2002**, *41*, 4718-4722; c) S. Trippett, *Phosphorus Sulfur*

1976, *1*, 89-98; d) S. Trippett, S. *Pure and Appl. Chem.* **1970**, *40*, 595-604; e) G. Buono, J. R. Llinas, *J. Am. Chem. Soc.* **1981**, *103*, 4532-4540; f) M. Eisenhut, H. L. Mitchell, D. D. Traficante, R. J. Kaufman, J. M. Deutsch, G. M. Whitesides, *J. Am. Chem. Soc.* **1974**, *96*, 5385-5397; g) C. G. Moreland, G. O. Doak, L. B. Littlefield, N. S. Walker, J. W. Gilje, R. W. Braun, A. H. Cowley, *J. Am. Chem. Soc.* **1976**, *98*, 2161-2165; h) L. V. Griend, R. G. Cavell, *Inorg. Chem.* **1983**, *22*, 1817-1820; i) S. Kumaraswamy, C. Muthiah, K. C. Kumara Swamy, *J. Am. Chem. Soc.* **2000**, *122*, 964-965; j) P. Kommana, S. Kumaraswamy, J. J. Vittal, K. C. Kumara Swamy, *Inorg. Chem.* **2002**, *41*, 2356-2363; k) P. Kommana, N. S. Kumar, J. J. Vittal, E. G. Jayasree, E. D. Jemmis, K. C. Kumara Swamy, *Org. Lett.* **2004**, *6*, 145-148.

[5] a) R. Hoffmann, J. M. Howell, E. L. Muetterties, *J. Am. Chem. Soc.* **1972**, *94*, 3047-3058; b) R. S. McDowell, A. Streitwieser Jr., *J. Am. Chem. Soc.* **1985**, *107*, 5849-5855; c) J. A. Deiters, R. R. Holmes, J. M. Holmes, *J. Am. Chem. Soc.* **1988**, *110*, 7672-7681; d) P. Wang, Y. Zhang, R. Glaser, A. E. Reed, P. v. R. Schleyer, A. Streitwieser, Jr., *J. Am. Chem. Soc.* **1991**, *113*, 55-64; e) H. Wasada, K. Hirao, *J. Am. Chem. Soc.* **1992**, *114*, 16-27; f) G. R. J. Thatcher, A. S. Campbell, *J. Org. Chem.* **1993**, *58*, 2272-2281; g) P. Wang, Y. Zhang, R. Glaser, A. Streitwieser, P. v. R.

Schleyer, *J. Comput. Chem.* **1993**, *14*, 522-529; h) B. D. Wladkowski, M. Krauss, W. J. Stevens, *J. Phys. Chem.* **1995**, *99*, 4490-4500.

[6] R. S. Berry, *J. Chem. Phys.* **1960**, *32*, 933-938.

[7] a) K. Mislow, *Acc. Chem. Res.* **1970**, *3*, 321-331; b) E. L. Muetterties, *Acc. Chem. Res.* **1970**, *3*, 266-273; c) I. Ugi, D. Marquarding, H. Klusacek, P. Gillespie, F. Ramirez, *Acc. Chem. Res.* **1971**, *4*, 288-296; d) P. Gillespie, P. Hoffman, H. Klusacek, D. Marquarding, S. Pfohl, F. Ramirez, E. A. Tsolis, I. Ugi, *Angew. Chem. Int. Ed.* **1971**, *10*, 687-715.

[8] J. Moc, K. Morokuma, *J. Am. Chem. Soc.* **1995**, *117*, 11790-11797.

[9] J. C. Martin, *Science* **1983**, *221*, 509-514.

[10] a) S. Kojima, K. Kajiyama, K.-y. Akiba, *Tetrahedron Lett.* **1994**, *35*, 7037-7040; b) S. Kojima, K. Kajiyama, K.-y. Akiba, *Bull. Chem. Soc. Jpn.* **1995**, *68*, 1785-1797.

[11] a) S. Kojima, K. Kajiyama, M. Nakamoto, K.-y. Akiba, *J. Am. Chem. Soc.* **1996**, *118*, 12866-12867; b) S. Kojima, K. Kajiyama, M. Nakamoto, S. Matsukawa, K.-y. Akiba, *Eur. J. Org. Chem.* **2006**, 218-234.

[12] a) K. Kajiyama, M. Yoshimune, M. Nakamoto, S. Matsukawa, S. Kojima, K.-y. Akiba, *Org.*

Lett. **2001**, *3*, 1873-1875; b) K. Kajiyama, M. Yoshimune, S. Kojima, K.-y. Akiba, *Eur*. *J*. *Org*. *Chem*. **2006**, 2739-2746.

[13] Some compounds which violates the apicophilicity concept were isolated. In these cases, some sort of steric constraints disallowed regular configulations. a) J. Kobayashi, K. Goto, T. Kawashima, *J. Am. Chem. Soc.* **2001**, *123*, 3387-3388; b) J. Kobayashi, K. Goto, T. Kawashima, M. W. Schmidt, S. Nagase, *J. Am. Chem. Soc.* **2002**, *124*, 3703-3712; c) S. Vollbrecht, A. Vollbrecht, J. Jeske, P. G. Jones, R. Schmutzler, W.-W. du Mont, *Chem. Ber./Recl/* **1997**, *130*, 819-822.

[14] a) K. C. Kumara Swamy, N. S. Kumar, *Acc. Chem. Res.* **2006**, *39*, 324-333; b) K. V. P. P. Kumar, N. S. Kumar, K. C. Kumara Swamy, *New J. Chem.* **2006,** *30*, 717-728; c) A. Chandrasekaran, N. V. Timosheva, R. R. Holmes, *Phosphorus, Sulfur, and Silicon and the Related Elements* **2006**, *181*, 1493-1511; d) N. S. Kumar, P. Kommana, J. J. Vittal, K. C. Kumara Swamy, *J. Org. Chem.* **2002**, *67*, 6653-6658.

[15] S. Matsukawa, S. Kojima, K. Kajiyama, Y. Yamamoto, K.-y. Akiba, S. Re, S. Nagase, *J*. *Am*. *Chem*. *Soc*. **2002**, *124*, 13154-13170.

[16] T. Adachi, S. Matsukawa, M. Nakamoto, K. Kajiyama, S. Kojima, Y. Yamamoto, K.-y. Akiba, S. Re, S. Nagase, *Inorg. Chem.* **2006**, *45*, 7269-7277.

[17] a) P. G. Gassman, N. J. O'Reilly, *J. Org. Chem.* **1987**, *52*, 2481-2490; b) V. A. Petrov, *Tetrahedron Lett.* **2001**, *42*, 3267-3269.

[18] for a review of the Cannizzaro reaction, see T. A. Geissman, *Org. React.* **1944**, *2*, 94-113.

[19] L. Jablonski, T. Billard, B. R. Langlois, *Tetrahedron Lett.* **2003**, *44*, 1055-1057.

[20] E. F. Perozzi, R. S. Michalak, G. D. Figuly, W. H. Stevenson III, D. B. Dess, M. R. Ross, J. C. Martin, *J. Org. Chem.* **1981**, *46*, 1049-1053.

[21] S. K. Chopra, J. C. Martin, *Heteroatom Chem.* **1991**, *2*, 71-79.

[22] The *D* angle, which is defined as a difference between the two largest angles around the central atom of pentacoordinate compound, were calculated for **3b**, **4b**, **9a**, **9b**, **9c**, **10a** and **10b** to be 46.4, 48.8, 50.3, 49.6, 48.5, 32.2 and 36.7˚, respectively. Considering the definition {$D \leq 15$˚: square pyramid (SP), $D \geq 45$˚: trigonal bipyramid (TBP)}, the geometries of **10a** and **10b** are intermediate case. However, the bond lengths for both compounds are very similar to **4b**; therefore, we regard all the phosphoranes cited in Table 1 as distorted TBP. For the *D* angle, see

a) K. Seppelt, in *Heteroatom Chemistry* (Ed.: E. Block), VCH Verlagsgesell schaft, Weinheim, Germany, **1990**, p. 335; b) A. Schmuck, D. Leopold, K. Seppelt, *Chem. Ber.* **1989**, *122*, 803-808; c) A. Schmuck, P. Pyykkoe, K. Seppelt, *Angew. Chem. Int. Ed. Engl.* **1990**, *29*, 213-215; d) A. Schmuck, D. Leopold, S. Wallenhauer, K. Seppelt, *Chem. Ber.* **1990**, *123*, 761-766.

[23] Otwinowski, Z. University of Texas, Southwestern Medical Center.

[24] Sheldrick, G. M. *SHELX-97*; University of Göttingen: Göttingen, Germany, 1997.

Figure and Scheme Legends

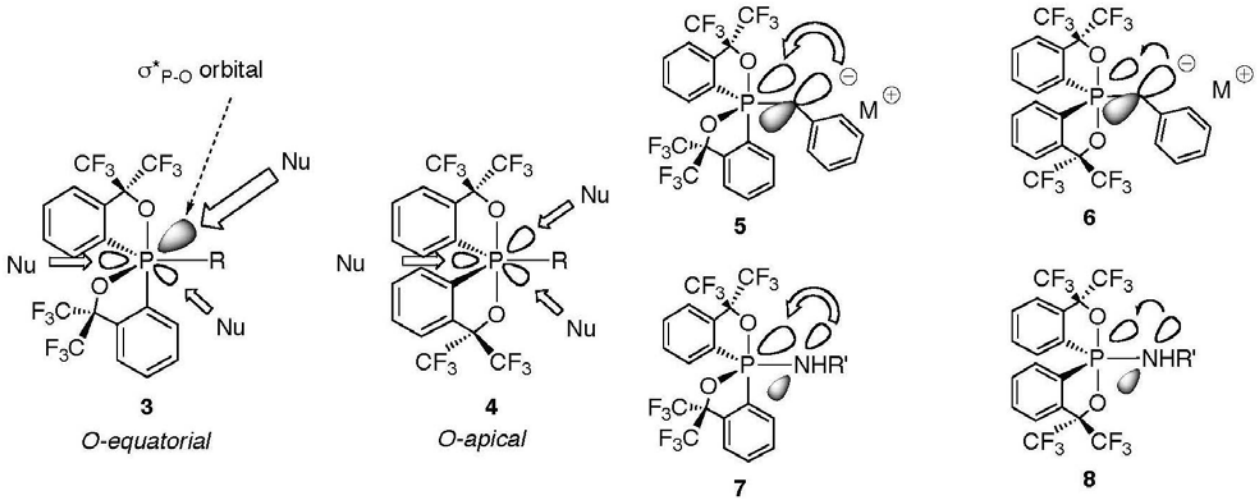

Figure 1. Enhanced electrophilicity of *O-equatorial* phosphorane (**3**) and the increased stability of the carbanion (**5**) and aminophosphorane (**7**) originated by the low-lying $\sigma^*_{P\text{-}O}$ orbitals in the equatorial plane

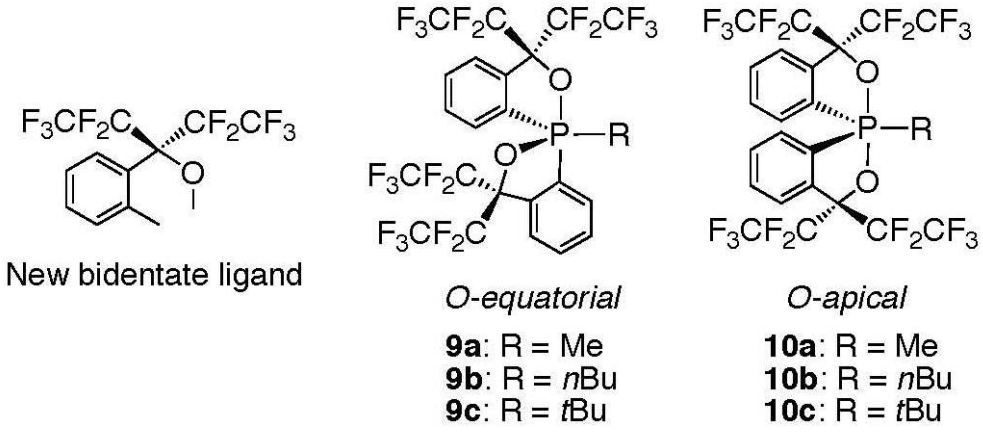

Figure 2. Spirophosphoranes bearing new bidentate ligands.

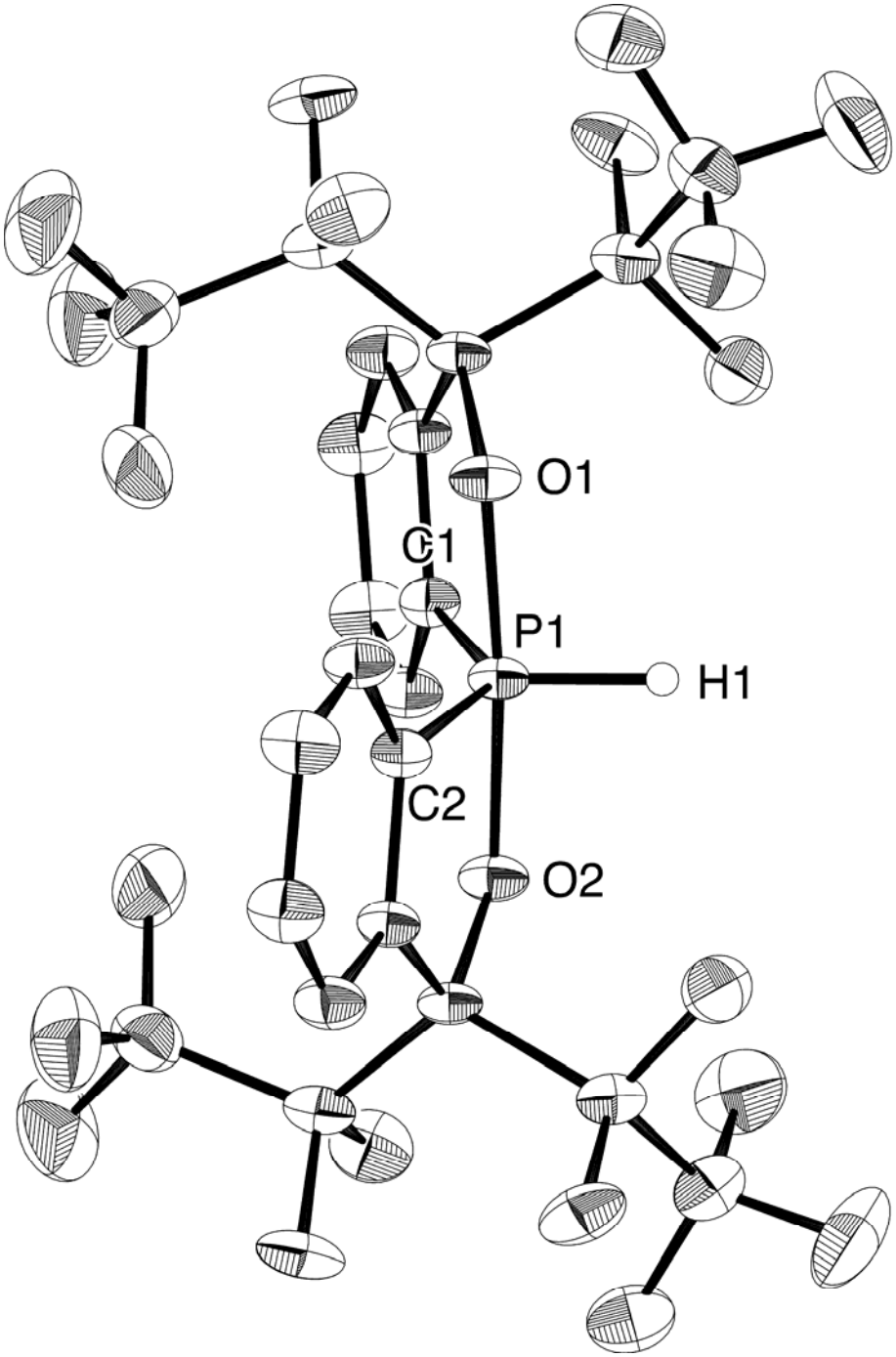

Figure 3. The ORTEP drawing of hydrophosphorane **16** showing the thermal ellipsoids at the 30% probability level. All the hydrogen atoms other than H1 have been omitted for clarity. Selected bond lengths [Å] and angles [˚]: P1—O1, 1.736(3); P1—O2, 1.736(3); P1—C1, 1.823(4); P1—C2, 1.823(4); P1—H1, 1.330(7); O1—P1—O2, 175.00(3); O1—P1—C1, 90.33(17); O1—P1—C2, 87.79(16); O1—P1—H1, 92.52(14); O2—P1—C1, 87.79(16); O2—P1—C2, 90.33(17); O2—P1—H1, 92.52(14); C1—P1—C2, 136.30(3); C1—P1—H1, 111.85(16); C2—P1—H1, 111.85(16).

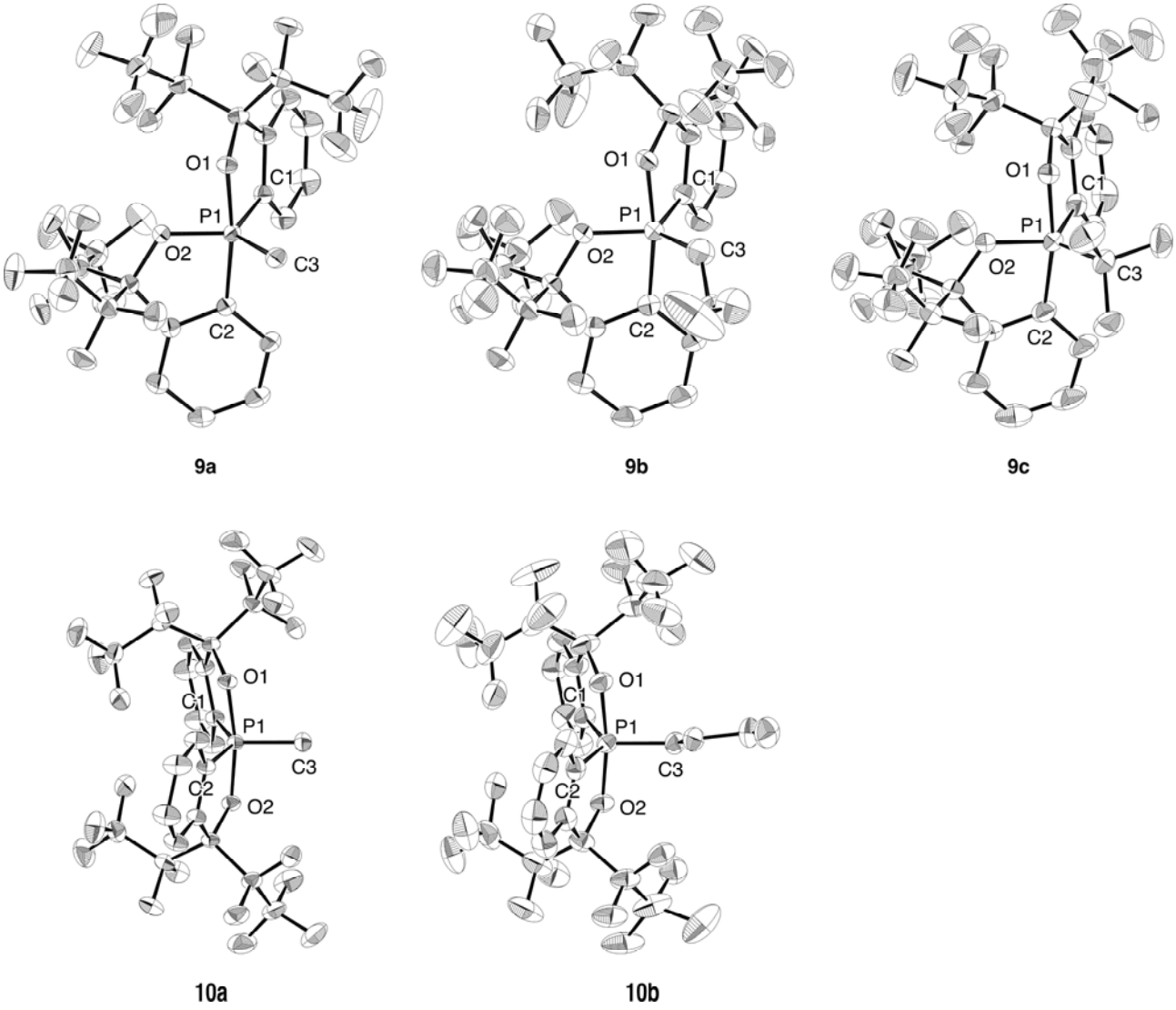

Figure 4. The ORTEP drawings of phosphoranes **9a**-**9c**, **10a** and **10b** showing the thermal ellipsoids at the 30% probability level. All the hydrogen atoms have been omitted for clarity.

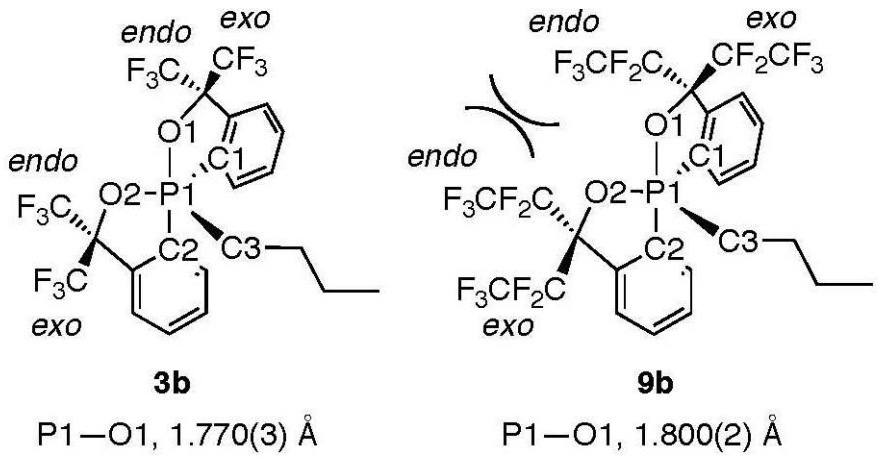

Figure 5. Steric repulsion of *endo*-C_2F_5 groups in the crystal structure of **9b**.

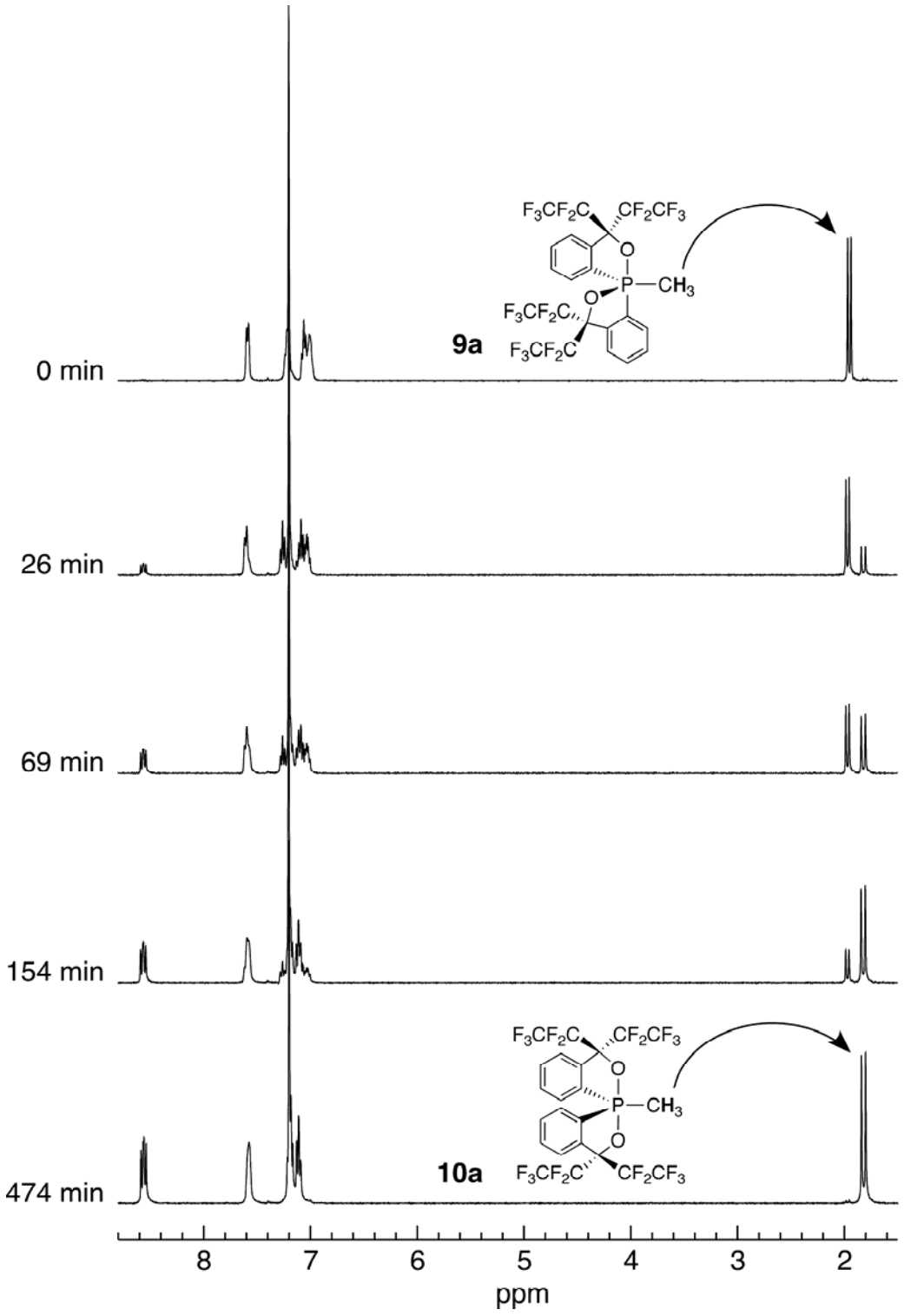

Figure 6. Time course of the ^{1}H NMR signals of the isomerization of **9a** to **10a** in C_6D_6 at 70 ˚C.

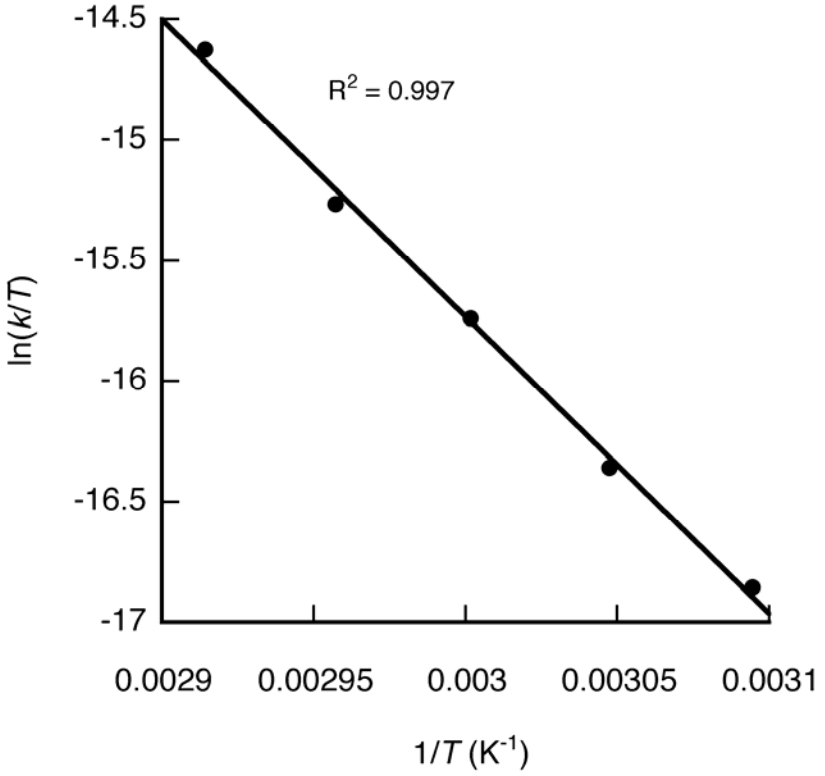

Figure 7. Eyring plot for the isomerization of **9a** to **10a**.

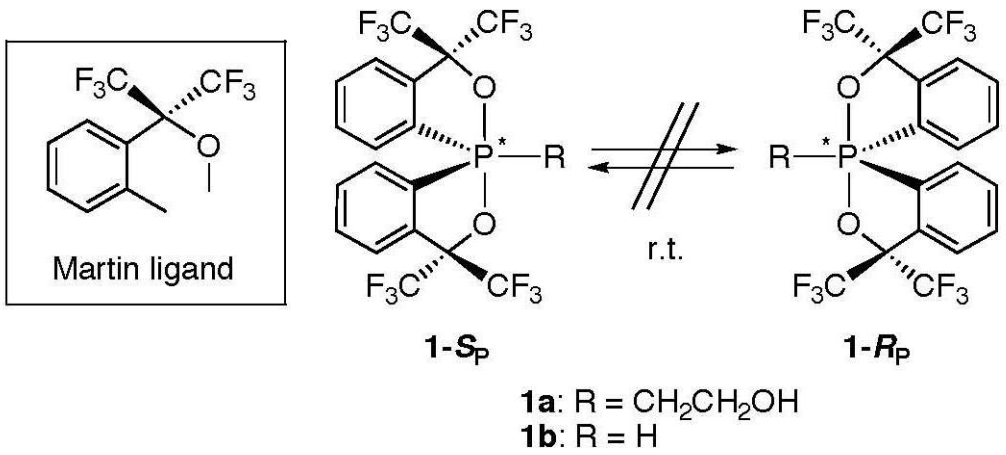

Scheme 1. Isolated enantiomeric pairs of optically active spirophosphoranes bearing the Martin ligands.

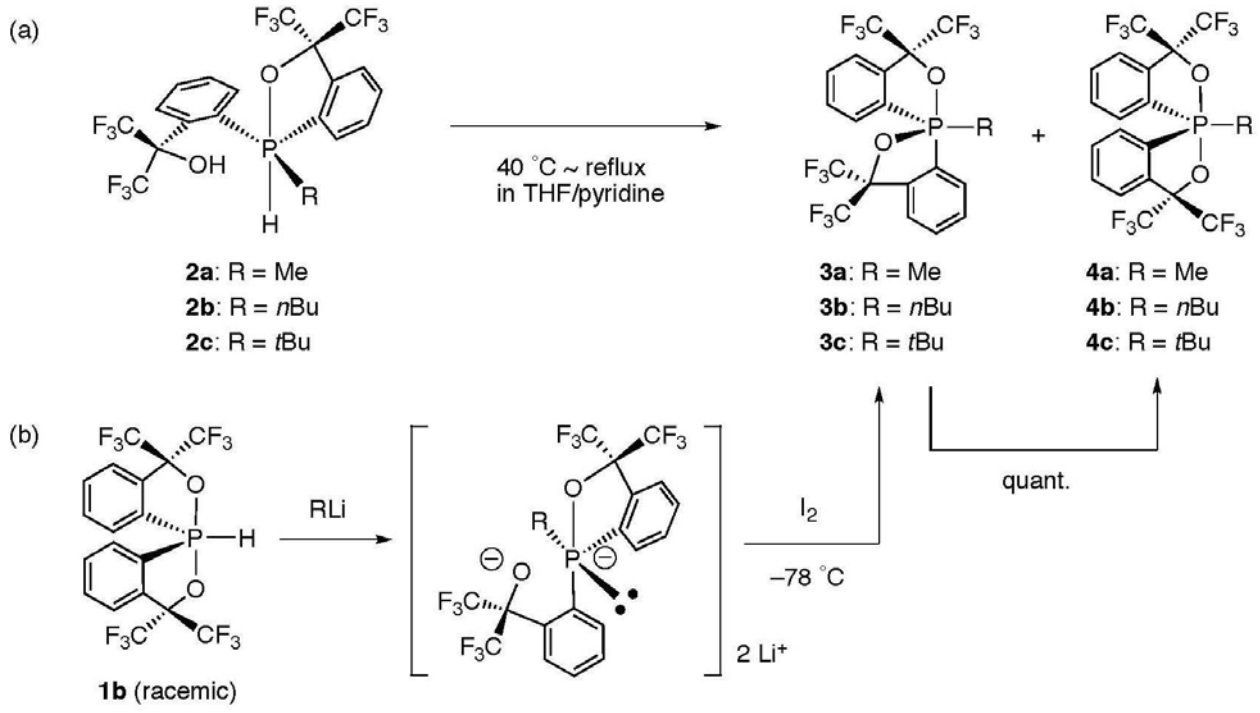

method	formation ratio 3a : 4a	3b : 4b	3c : 4c
a	53 : 47	71 : 29	>99 : <1
b	>99 : <1	>99 : <1	>99 : <1

Scheme 2. Preparation of *O-equatorial* spirophosphoranes **3** and *O-apical* isomers **4**. (a) via dehydrogenative cyclization, and (b) oxidation of dianionic phosphorane.

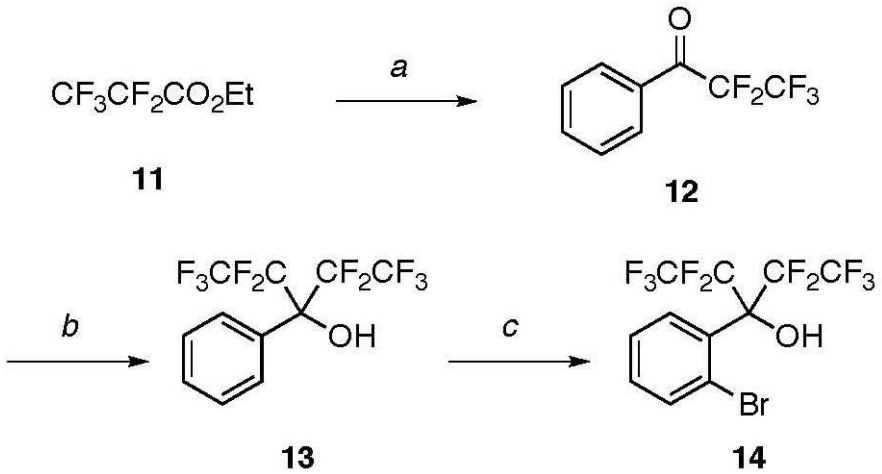

Scheme 3. Synthesis of **13** and **14**. Reagents, conditions and yields: (a) PhLi (1.1 equiv.), THF, –78 ˚C, 2 h; then 2 M HCl, 84%; (b) *t*BuOK (0.5 equiv.), THF, r.t., 15 h; then CF_3COOH, CH_2Cl_2, 33%; (c) *n*BuLi/TMEDA (3.0 equiv./3.0 equiv.), hexane, r.t., 36 h; then $BrCF_2CF_2Br$ (4.5 equiv.), r.t., 3 h,

84%.

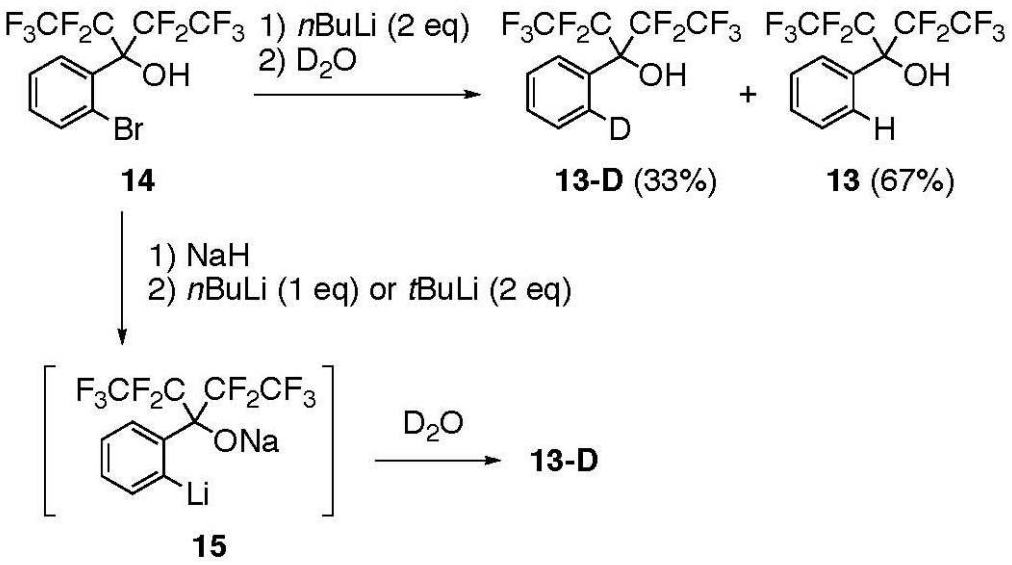

Scheme 4. Examination of dimetallation of **14**.

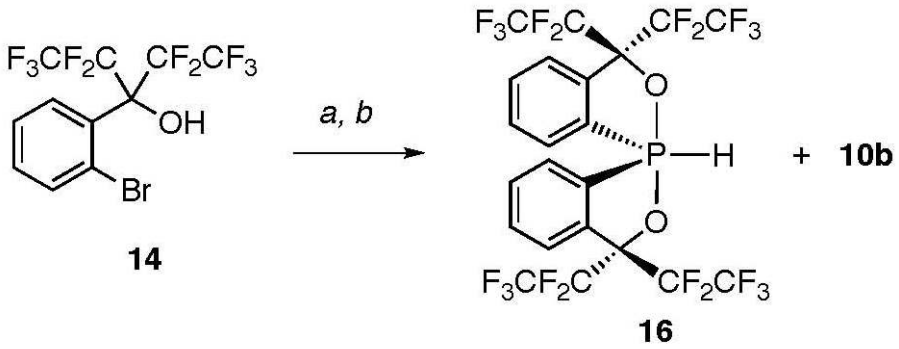

Scheme 5. Synthesis of hydrophosphorane **16**. Reagents, conditions and yields: (a) NaH (2.0 equiv.), 0 ˚C, 0.5 h, THF; then *n*BuLi (1.0 equiv.), –78 ˚C, 1 h, r.t., 1 h; (b) PCl_3 (0.5 equiv.), –78 ˚C, 0.5 h, 0 ˚C, 1.5 h; then 6 M HCl, **16**: 50%, **10b**: 6%.

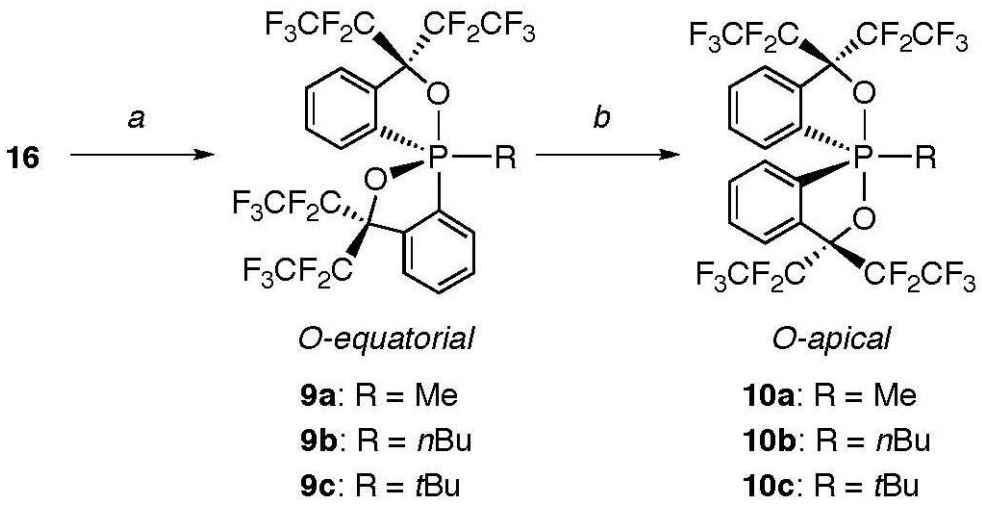

Scheme 6. Synthesis of *O-equatorial* spirophosphoranes **9**, and isomerization of **9** to **10**. Reagents, conditions and yields: (a) RLi (3.0 equiv.), Et_2O, r.t., 3 h; then I_2 (3.0 equiv.), –78 ˚C to r.t., 3 h, **9a**: 90%, **9b**: 92%, **9c**: 43%; (b) C_6D_6, 75 ˚C, 8 h, **10a**: 98%; C_6D_6, 80 ˚C, 12 h, **10b**: 100%; diglyme, 195 ˚C, 3 weeks, **10c**: 92%.

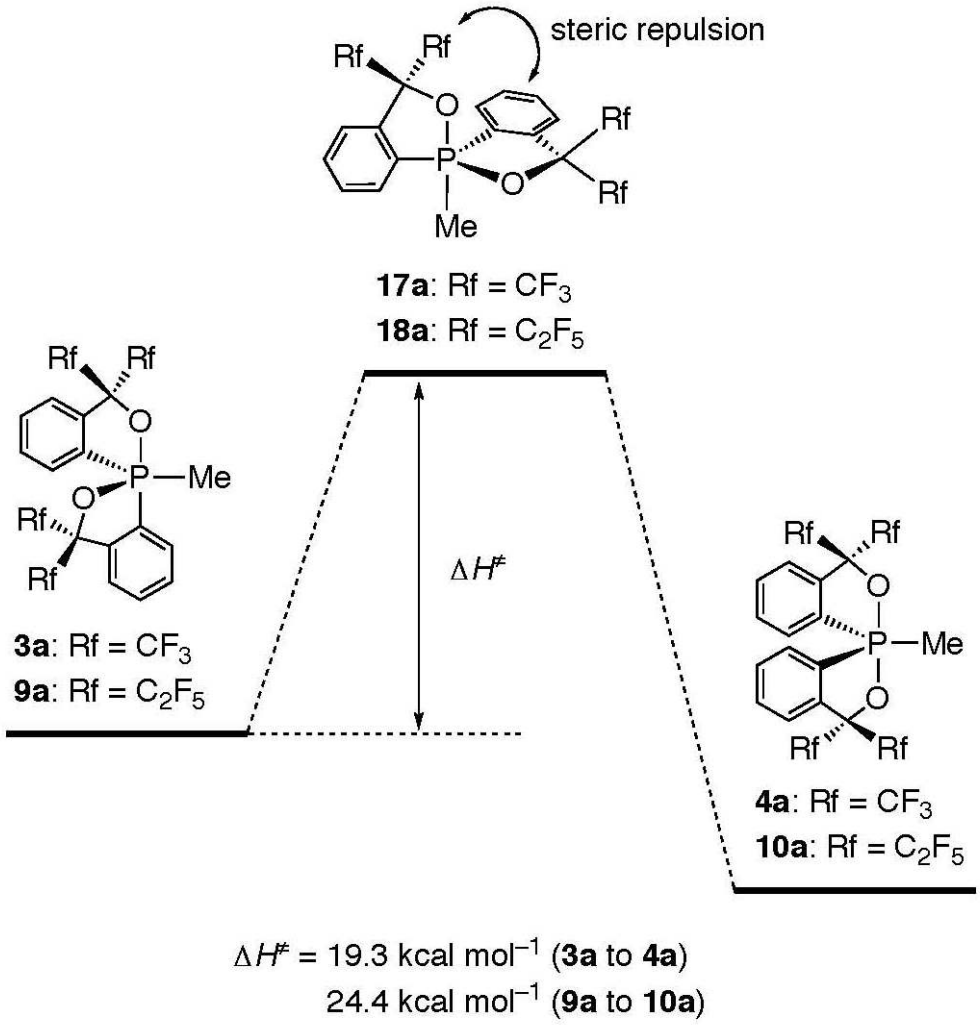

Scheme 7. Energy diagram of the isomerization of *O-equatorial* phosphorane to the *O-apical* isomer.

Tables

Table 1. Selected bond lengths [Å] and angles [°] for **9a-9c**, **10a-10b**, **3b**[11a] and **4b**.[11a]

Compound	**9a**	**9b**	**9c**	**10a**	**10b**	**3b**[11a]	**4b**[11a]
P1—O1	1.7858(17)	1.800(2)	1.8031(15)	1.7588(12)	1.759(3)	1.770(3)	1.763(1)
P1—O2	1.6547(17)	1.661(2)	1.6639(15)	1.7588(12)	1.750(3)	1.660(3)	1.754(1)
P1—C1	1.827(2)	1.828(3)	1.837(2)	1.8320(17)	1.829(4)	1.810(4)	1.816(1)
P1—C2	1.879(2)	1.864(3)	1.886(2)	1.8320(17)	1.824(4)	1.866(4)	1.817(1)
P1—C3	1.814(3)	1.841(4)	1.902(2)	1.810(3)	1.826(4)	1.832(5)	1.818(1)
O1—P1—O2	83.89(8)	83.27(9)	82.94(7)	169.32(9)	170.95(13)	82.8(2)	175.8(1)
O1—P1—C1	86.38(9)	86.11(11)	85.21(8)	89.29(7)	86.62(15)	87.4(2)	87.3(1)
O1—P1—C2	171.58(10)	170.97(12)	169.76(9)	86.80(7)	90.16(16)	170.5(2)	90.6(1)
O1—P1—C3	88.55(11)	88.94(17)	88.90(9)	95.34(5)	93.37(16)	88.7(2)	91.2(1)
O2—P1—C1	119.52(10)	119.67(13)	118.02(9)	86.80(7)	89.49(14)	120.1(2)	91.0(1)
O2—P1—C2	87.92(9)	87.70(12)	87.21(9)	89.29(7)	86.71(15)	87.8(2)	87.3(1)
O2—P1—C3	117.97(11)	117.58(19)	119.06(10)	95.34(5)	95.67(15)	124.1(2)	93.0(1)
C1—P1—C2	99.42(11)	98.46(13)	97.02(10)	137.10(12)	134.28(16)	98.8(2)	127.0(1)
C1—P1—C3	121.27(12)	121.4(2)	121.26(11)	111.45(6)	112.73(17)	114.5(2)	116.5(1)
C2—P1—C3	93.57(12)	95.23(18)	98.37(11)	111.45(6)	112.98(16)	95.2(2)	116.5(1)

Table 2. Crystallographic data for **16** and **9a**-**9c**, **10a** and **10b**.

Compound	**16**	**9a**	**10a**
Formula	$C_{22}H_9F_{20}O_2P$	$C_{23}H_{11}F_{20}O_2P$	$C_{23}H_{11}F_{20}O_2P$
Mol wt	716.26	730.29	730.29
Cryst syst	monoclinic	monoclinic	orthorhombic
Space group	*C*2/*c*	$P2_1/c$	*Pbcn*
Color	colorless	colorless	colorless
Habit	plate	plate	plate
Cryst dimens, mm	0.60 × 0.60 × 0.60	0.40 × 0.40 × 0.40	0.50 × 0.20 × 0.20
a, Å	9.2910(3)	11.5700(2)	18.7160(5)
b, Å	14.4960(5)	13.6760(3)	8.3700(10)
c, Å	19.3220(8)	16.8200(4)	17.0800(4)
α, deg	90	90	90
β, deg	102.2320(10)	98.4340(10)	90
γ, deg	90	90	90
V, Å^3	2543.25(16)	2632.67(10)	2675.63(10)
Z	4	4	4
Dcalc, g cm^{-3}	1.871	1.842	1.813
Abs coeff, mm^{-1}	0.277	0.270	0.266
F(000)	1408	1440	1440
Radiation; λ, Å	Mo *K*α, 071073	Mo *K*α, 071073	Mo *K*α, 071073
Temp, K	298(2)	298(2)	298(2)
Data,collcd	+*h*, +*k*, ±*l*	+*h*, +*k*, ±*l*	+*h*, +*k*, +*l*
Data/restrains/para	2594/0/206	5958/0/416	3169/0/210
R_1 [$I > 2\sigma(I)$]	0.0737	0.0649	0.0580
wR_2 (all data)	0.2470	0.2034	0.1750
GOF	1.197	1.074	1.123
Solv for crystallization	*n*-hexane/ether	CH_3CN	$CHCl_3$

Table 2 (continued)

Compound	**9b**	**10b**	**9c**
Formula	$C_{26}H_{17}F_{20}O_2P$	$C_{26}H_{17}F_{20}O_2P$	$C_{26}H_{17}F_{20}O_2P$
Mol wt	772.37	772.37	772.37
Cryst syst	monoclinic	triclinic	Monoclinic
Space group	$P2_1/c$	$P\bar{1}$	$P2_1/c$
Color	colorless	colorless	Colorless
Habit	plate	plate	Plate
Cryst dimens, mm	0.50 × 0.20 × 0.20	0.90 × 0.70 × 0.50	0.50 × 0.40 × 0.40
a, Å	8.8950(2)	9.678(3)	12.6860(2)
b, Å	19.7730(4)	10.044(6)	12.9690(2)
c, Å	17.1150(5)	16.385(5)	18.6730(4)
α, deg	90	103.63(4)	90
β, deg	103.1120(10)	95.28(2)	109.0380(10)
γ, deg	90	101.18(4)	90
V, Å^3	2931.72(12)	1502.6(11)	2904.13(9)
Z	4	2	4
Dcalc, g cm^{-3}	1.750	1.707	1.767
Abs coeff, mm^{-1}	0.248	0.242	0.250
F(000)	1536	768	1536
Radiation; λ, Å	Mo *K*α, 071073	Mo *K*α, 071073	Mo *K*α, 071073
Temp, K	298(2)	298(2)	298(2)
Data,collcd	$+h, +k, \pm l$	$\pm h, -k, \pm l$	$+h, +k, \pm l$
Data/restrains/para	6519/0/479	5251/0/503	6965/0/537
R_1 [$I > 2\sigma(I)$]	0.0758	0.0927	0.0688
wR_2 (all data)	0.2541	0.3155	0.2089
GOF	1.095	1.471	1.055
Solv for crystallization	CH_3CN	$CHCl_3$	$CHCl_3$

Table 3. Rate constants and activation parameters for stereomutation from **9a** to **10a**.

Temp. [K]	k [s^{-1}]	$\Delta G^{\neq}$ [kcal mol^{-1}]	$\Delta H^{\neq}$ [kcal mol^{-1}]	$\Delta S^{\neq}$ [e.u.]
323	$(1.51 \pm 0.01) \times 10^{-5}$	26.00		
328	$(2.55 \pm 0.02) \times 10^{-5}$	26.03		
333	$(4.76 \pm 0.03) \times 10^{-5}$	26.06	24.4 ± 0.8	–5.1 ± 2.4
338	$(7.70 \pm 0.06) \times 10^{-5}$	26.08		
343	$(15.0 \pm 0.18) \times 10^{-5}$	26.11		

Error is given as standard deviation.

Text for the Table of Contents

Frozen Berry pseudorotation: 1,1,1,2,2,4,4,5,5,5-Decafluoro-3-phenyl-3-pentanol (**13**) was prepared by the Cannizzaro-type reaction of the pentafluoropropiophenone. Phosphoranes exhibiting reversed apicophilicity (*O-equatorial*: **9**) were isolated in good yields utilizing novel bidentate ligand derived from **13**. Based on the kinetic study of stereomutation of the *O-equatorial* **9** to the *O-apical* **10**, remarkable steric effect of the C_2F_5 group for freezing Berry pseudorotation (BPR) was observed.

<Figure for TOC>

Keywords: Hypervalent compounds / Isomerization / Spirophosphorane / X-ray crystallography